JOURNAL OF VIROLOGY, Apr. 1995, p. 2016–2023 Vol. 69, No. 4
0022-538X/95/$04.00+0

Specific Binding of Host Cellular Proteins to Multiple Sites within the 3′ End of Mouse Hepatitis Virus Genomic RNA

WEI YU[1] AND JULIAN L. LEIBOWITZ[1,2]*

Department of Pathology and Laboratory Medicine[1] and Department of Microbiology and Molecular Genetics,[2] The University of Texas Medical School at Houston, Houston, Texas 77225

Received 29 September 1994/Accepted 21 December 1994

The initial step in mouse hepatitis virus (MHV) RNA replication is the synthesis of negative-strand RNA from a positive-strand genomic RNA template. Our approach to begin studying MHV RNA replication is to identify the *cis*-acting signals for RNA synthesis and the proteins which recognize these signals at the 3′ end of genomic RNA of MHV. To determine whether host cellular and/or viral proteins interact with the 3′ end of the coronavirus genome, an RNase T_1 protection/gel mobility shift electrophoresis assay was used to examine cytoplasmic extracts from mock- and MHV-JHM-infected 17Cl-1 murine cells for the ability to form complexes with defined regions of the genomic RNA. We demonstrated the specific binding of host cell proteins to multiple sites within the 3′ end of MHV-JHM genomic RNA. By using a set of RNA probes with deletions at either the 5′ or 3′ end or both ends, two distinct binding sites were located. The first protein-binding element was mapped in the 3′-most 42 nucleotides of the genomic RNA [3′ (+42) RNA], and the second element was mapped within an 86-nucleotide sequence encompassing nucleotides 171 to 85 from the 3′ end of the genome (171-85 RNA). A single potential stem-loop structure is predicted for the 3′ (+)42 RNA, and two stem-loop structures are predicted for the 171-85 RNA. Proteins interacting with these two elements were identified by UV-induced covalent cross-linking to labeled RNAs followed by sodium dodecyl sulfate-polyacrylamide gel electrophoresis analysis. The RNA-protein complex formed with the 3′-most 42 nucleotides contains approximately five host polypeptides, a highly labeled protein of 120 kDa and four minor species with sizes of 103, 81, 70, and 55 kDa. The second protein-binding element, contained within a probe representing nucleotides 487 to 85 from the 3′ end of the genome, also appears to bind five host polypeptides, 142, 120, 100, 55, and 33 kDa in size, with the 120-kDa protein being the most abundant. The RNA-protein complexes observed with MHV-infected cells in both RNase protection/gel mobility shift and UV cross-linking assays were identical to those observed with uninfected cells. The possible involvement of the interaction of host proteins with the viral genome during MHV replication is discussed.

Mouse hepatitis virus (MHV), a coronavirus, contains a large, single-stranded, polyadenylated genomic RNA of positive sense which is approximately 31 kb in length (12, 13, 29, 38). MHV utilizes a complex transcriptional strategy which is not completely understood. Several alternative models have been described to explain the mechanism of MHV RNA synthesis (9, 18, 34, 35). In all of these models, the initial step in MHV RNA replication is the synthesis of negative-strand RNA from a positive-strand genomic template.

One approach to studying MHV RNA synthesis is to identify *cis*-acting signals for RNA replication and the proteins which recognize these signals. Analysis of the structure of defective interfering (DI) RNAs (naturally occurring or constructed in vitro) indicated that approximately 470 nucleotides (nt) at the 5′ terminus, 436 nt at the 3′ terminus, and about 135 internal nt were required for DI RNA replication in MHV-infected cells and suggested that these sequences retain signals necessary for RNA replication (7, 21, 22). Studies to examine the effects of deletions at the 3′ region on DI RNA replication demonstrated that any deletion within the 436 nt at the 3′ end of the genome was lethal for DI RNA replication (7). A recent study has shown that a 55-kDa host cell protein bound to positive-sense RNA corresponding to nt 56 to 112 at the 5′ end of the genome but failed to demonstrate any protein binding to a 90-nt probe from the 3′ end of positive-strand genome (5).

We have focused our attention on the 3′ end of MHV genome. It is likely that the 3′ region contains sequences necessary for viral RNA polymerase binding and that recognition of the 3′ region of coronavirus RNA is carried out by viral and perhaps host cell proteins as well. To elucidate the molecular mechanism of MHV RNA replication mediated by the 3′ region of the genome, we have initiated studies to identify whether cellular and/or viral proteins form complexes with this region of genomic RNA, to localize protein-binding sites within this region, and to characterize binding proteins in RNA-protein complexes by RNase protection/gel mobility shift and UV cross-linking assays. MHV proteins binding to the 3′ end of virion RNA were sought by comparing the abilities of MHV-infected and uninfected cytoplasmic extracts to form complexes with synthetic RNA probes corresponding to 3′-end sequences. Here, we report the specific binding of host cellular proteins to two regions within 487 bases of the 3′ end of genomic RNA of MHV and the identification of different host proteins contributing to RNA binding. The binding of host proteins to the 3′ end of genomic RNA suggests the involvement of this interaction in the initial steps of MHV RNA replication.

* Corresponding author. Mailing address: Department of Pathology and Laboratory Medicine, P.O. Box 20708, University of Texas Health Sciences Center, Houston, TX 77225. Phone: (713) 792-8360. Fax: (713) 794-4149. Electronic mail address: leib@casper.med.uth.tmc.edu.

MATERIALS AND METHODS

Virus and cells. Murine 17Cl-1 cells were cultured with Dulbecco's minimal essential medium supplemented with 10% fetal bovine serum at 37°C in a 3%

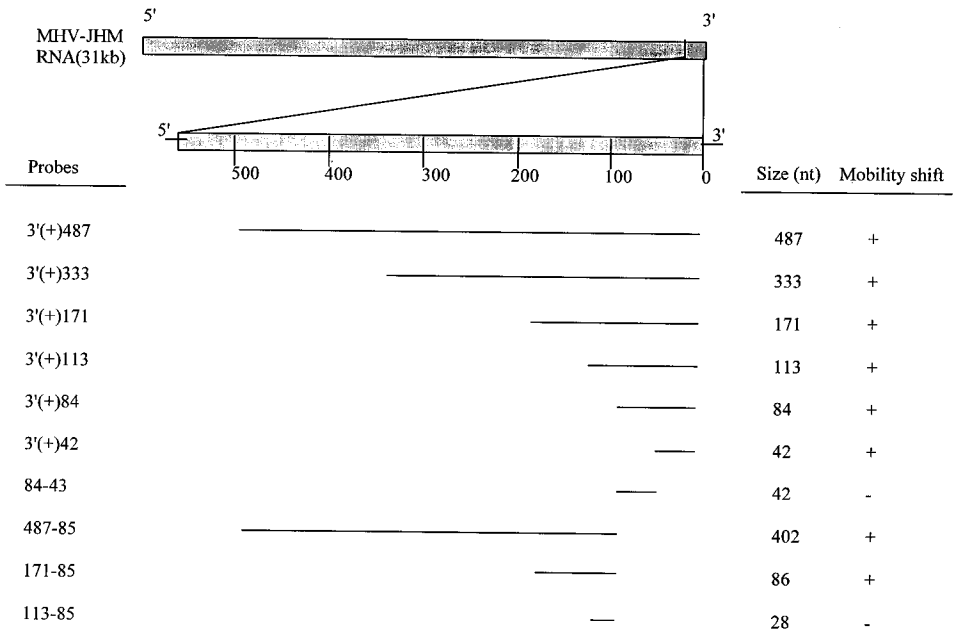

FIG. 1. Schematic diagram of the MHV genome, the locations of RNA probes, and summary of RNase T_1 protection/gel mobility shift assays. cDNAs representing various segments of the 3′ end of the MHV genome fused to the T7 promoter were synthesized as described in Materials and Methods. ^{32}P-labeled RNA probes were synthesized by in vitro transcription with T7 RNA polymerase. Each probe was named by nucleotide numbers or location within the genomic RNA sequence upstream from the 5′-most A in the poly(A) tail (position 0). For example, probe 3′ (+)487 represents the 487 nt upstream from 0, and probe 171-85 represents an 86-nt sequence from nt 171 to 85 upstream from position 0. The size of each probe is indicated, as are the relative position and length. +, formation of an RNase-resistant complex; −, no complex was detected in RNase protection/mobility shift assays.

CO_2 atmosphere (16, 37). The origin and growth of the MHV-JHM strain used in this study have been described elsewhere (16).

Preparation of mock- and MHV-JHM-infected cytoplasmic extracts. Cytoplasmic extracts from both uninfected and virus-infected cells were prepared according to a previously described protocol, with some minor modifications (3, 40). Virus-infected cytoplasmic extracts were prepared from 17Cl-1 cells inoculated with MHV-JHM at a multiplicity of infection of 3 and harvested after incubation at 37°C for 6.5 to 7 h. Cells, either infected with MHV or uninfected, were washed twice with cold phosphate-buffered saline, scraped, and centrifuged at 500 × *g* for 5 min. Cell pellets were resuspended in a hypotonic buffer (10 mM *N*-2-hydroxyethylpiperazine-*N*′-2-ethanesulfonic acid [HEPES; pH 7.6], 1.5 mM $MgCl_2$, 10 mM KCl, 0.2 mM phenylmethysulfonyl fluoride) and held on ice for 5 min. Cells were lysed by adding Nonidet P-40 to a final concentration of 0.5%, vortexed, and checked for lysis by observation under a light microscope. Nuclei were removed by centrifugation at 4,000 × *g* at 4°C for 15 min. The supernatant was brought to 5% glycerol and stored at −80°C. The protein concentration was determined with a Bio-Rad protein assay kit.

Design of primers and in vitro synthesis of RNA transcripts. The strategy used to synthesize cDNA fragments representing the 3′ end of the JHM genome and generate the RNA transcripts throughout this study is outlined in Fig. 1. A series of 5′-end primers (positive sense) containing the T7 RNA polymerase promoter (TAA TAC GAC TCA CTA TAG GGC GAG) was synthesized. A series of 3′-end negative sense primers was similarly synthesized. A double-stranded cDNA, p118-8a, representing 1,648 nt from the 3′ end of JHM genomic RNA (15) was used as a DNA template for PCR. PCR products of defined size were synthesized by *Taq* DNA polymerase (Promega) and purified with either the Wizard PCR Prep kit (Promega) or the Mermaid kit (Bio 101) or by gel filtration through a Sephadex G-50 (Sigma) column. The primer pairs and the corresponding probes which were subsequently transcribed from the resulting PCR products are described in Table 1.

In vitro transcription reactions of PCR product templates by T7 RNA polymerase (Promega) were carried out as described by the manufacturer. The nucleotide concentrations were 0.5 mM for ATP, CTP, and GTP and 0 to 12.5 μM for UTP. Transcripts were uniformly labeled with 350 to 500 μCi of [^{32}P]UTP (3,000 Ci/mmol; ICN) in the presence of RNasin (Promega). Transcription reaction mixtures were then treated with RNase-free DNase (Promega) and extracted twice with phenol-chloroform. Unincorporated nucleotides were removed by gel filtration through a Sephadex G-50 column. The specific activities of transcripts were approximately 1×10^8 to 7×10^8 cpm/μg. To examine the purity of RNA probes synthesized prior to their use in RNase protection/mobility shift assays, aliquots of several labeled transcripts, for example, 3′ (+)487, 3′ (+)333, 3′ (+)113, and 3′ (+)84, in 1× Tris-acetate-EDTA buffer were denatured by heating at 65°C for 1 h, electrophoresed on 1% agarose gels, and autoradiographed. Each probe yielded a single homogeneous band (data not shown).

RNase T_1 protection and gel mobility shift electrophoresis assays. Binding reactions were performed in a volume of 10 μl as described previously (19, 40), with some modification. Cytoplasmic lysates containing 7 μg of protein and 1 to 2 ng of ^{32}P-labeled RNA probes were incubated at 22°C for 20 min in a buffer containing 50 mM KCl, 10 mM HEPES (pH 7.6), 2.5 mM $MgCl_2$, 1 mM dithio-

TABLE 1. Probes and primers synthesized

Probe	Positive-sense 5′ primer	Negative-sense 3′ primer
3′ (+)487	PT7-GAG AAA GAG AGG GAC AAA GC	GTG ATT CTT CCA ATT GGC
3′ (+)333	PT7-CCA GAT GGG TTA GAA GAT GAC	GTG ATT CTT CCA ATT GGC
3′ (+)171	PT7-TTA GTT GAA AGA GAT TGC	GTG ATT CTT CCA ATT GGC
3′ (+)113	PT7-TCT AAC CAT AAG AAC GGC	GTG ATT CTT CCA ATT GGC
3′ (+)84	PT7-CCT GGG AAG AGC TCA CAT	GTG ATT CTT CCA ATT GGC
3′ (+)42	PT7-TAG TAA ATG AAT GAA GTT	GTG ATT CTT CCA ATT GGC
84-43	PT7-CCT GGG AAG AGC TCA CAT	GGG CAT TGC AGG AAT AGT A
487-85	PT7-GAG AAA GAG AGG GAC AAA GC	GGG CGC CTA TCG CCG TT
171-85	PT7-TTA GTT GAA AGA GAT TGC	GGG CGC CTA TCG CCG TT
113-85	PT7-TCT AAC CAT AAG AAC GGC	GGG CGC CTA TCG CCG TT

threitol, and 9% glycerol. Ten micrograms of heparin (Sigma) and 500 ng of poly(I)-poly(C) (Boehringer Mannheim) were included to reduce nonspecific binding. For competition assays, unlabeled specific and nonspecific competitor RNAs were dried in the reaction tubes prior to addition of the reaction components. Reaction mixtures containing RNA-protein complexes and unbound RNAs were digested at 22°C for 20 min by RNase T_1 (Calbiochem) at different concentrations as indicated in figure legends. RNA-protein complexes were electrophoresed on a 6% nondenaturing polyacrylamide gel (acrylamide/bisacrylamide ratio, 60:1) in 0.5× Tris-borate-EDTA at 210 V in the cold room. Gels were dried and autoradiographed.

UV-induced cross-linking of RNA-protein complexes. For UV cross-linking of RNA and protein, the reaction mixtures were put on ice after RNase T_1 digestion and exposed to UV light (254 nm; Hoefer UVC 1000) at a 10-cm distance for 30 min. Twenty micrograms of RNase A (Sigma) was added, and the mixture was incubated for 30 min at 37°C to completely digest unlinked RNAs. The samples were analyzed by electrophoresis on 12% polyacrylamide gels containing sodium dodecyl sulfate (SDS). The gels were fixed, dried, and autoradiographed.

RESULTS

Identification of specific proteins binding to the 3′ end of genomic JHM RNA. Analysis of the structure of synthetic DI RNAs indicated that at least 436 nt corresponding to the 3′ terminus of the genome were required for DI RNA replication in the presence of helper virus (21). The apparent requirement for as many as 436 nt at the 3′ end of MHV DI RNAs suggests that a sequence within this region would retain signals required to bind viral and/or host proteins necessary for negative-strand RNA synthesis (7, 21). To investigate this hypothesis, we have performed a series of RNase T_1 protection/gel retardation assays. The first RNA probe selected for binding reactions corresponded to the 487 nt at the 3′ end of the MHV-JHM genome and spans the minimal length (436 nt) of the 3′ region required for MHV DI replication (21). A cDNA containing the last 487 bases of the 3′ end of the MHV-JHM genome (not including the polyadenylate tail) under the control of the T7 promoter was synthesized by PCR as shown in Fig. 1. ^{32}P-labeled RNA was transcribed from this template by T7 RNA polymerase. Cytoplasmic extracts prepared from both JHM-infected and uninfected 17Cl-1 cells were incubated with 2 ng of labeled probe in the presence of heparin and poly(I)-poly(C) to decrease nonspecific binding. In a series of preliminary experiments, reaction mixtures containing this 487-nt RNA transcript were displayed by electrophoresis on nondenaturing agarose or polyacrylamide gels. These experiments proved unsatisfactory because of poor resolution. Complexes formed with the 3′ (+)487 probe run on 4, 5, or 6% polyacrylamide gels, or on agarose gels, yield a smear of RNA-protein complexes poorly resolved from free probe (data not shown). The addition of an RNase T_1 digestion step prior to electrophoresis increases both the resolution and the sensitivity of gel shift assays by digesting unbound RNA and RNA nonspecifically bound to protein and by decreasing the size and apparent heterogeneity of the RNA-protein complexes (14). Thus, after allowing formation of RNA-protein complexes, we subjected the reactions to limited digestion with RNase T_1 (0.05 U per reaction) prior to electrophoresis. RNase T_1-resistant RNA-protein complexes were electrophoresed on 6% nondenaturing polyacrylamide gels and visualized by autoradiography. Incubation of the 3′ (+)487 probe with mock- or JHM-infected cell lysates protected a portion of the probe from T_1 digestion, resulting in two stable, poorly resolved, RNase T_1-resistant complexes, as shown in Fig. 2. The complexes formed by the 3′ (+)487 probe with cytoplasmic extracts from either mock-infected (Fig. 2, lane 2) or JHM-infected (Fig. 2, lane 9) cells appeared to have identical electrophoretic mobilities.

To verify the specificity of the RNA-protein binding, competition experiments with 50- and 100-fold molar excesses of unlabeled specific and nonspecific competitor RNAs were performed. The formation of the two T_1-resistant complexes by the 3′ (+)487 probe was greatly inhibited by a 50-fold molar excess of the unlabeled 3′ (+)487 RNA (Fig. 2, lanes 3 [uninfected cells] and 10 [MHV-infected cells]) and was completely blocked by a 100-fold molar excess of unlabeled 3′ (+)487 RNA (Fig. 2, lanes 4 [uninfected cells] and 11 [MHV-infected cells]). Only a slight diminution of binding was observed with unlabeled nonspecific competitor RNAs, including a 50- to 100-fold molar excess of 75- to 90-nt tRNA (Fig. 2, lanes 5 and 6 [uninfected cells] and 12 and 13 [MHV-infected cells]) and a 294-nt synthetic transcript corresponding to the 5′ end of the MHV-A59 genome (Fig. 2, lanes 7 and 8 [uninfected cells] and 14 and 15 [MHV-infected cells]). Furthermore, no bands corresponding to the complexes were observed when the 3′ (+)487 probe alone was digested with RNase T_1 in the absence of cytoplasmic lysate (Fig. 2, lane 1).

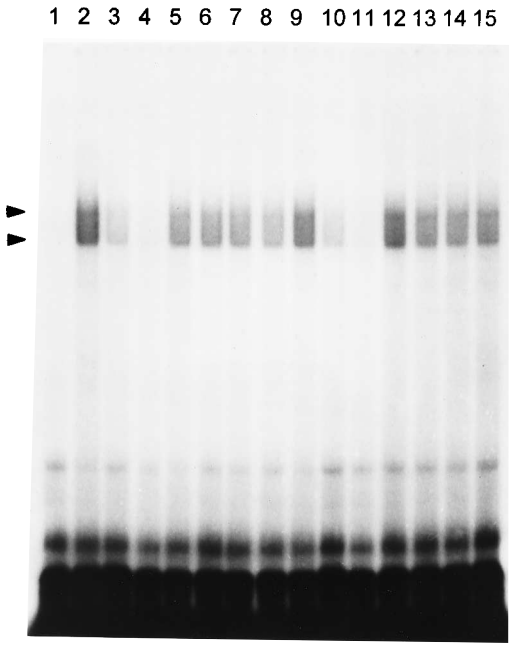

FIG. 2. Specific binding of host cellular proteins to the 3′ end of MHV-JHM genomic RNA. Two nanograms of ^{32}P-labeled 3′ (+)487 RNA was incubated with cytoplasmic extracts from either mock-infected (lanes 2 to 8) or MHV-JHM-infected (lanes 9 to 15) 17Cl-1 cells as described in Materials and Methods. Some samples contained competitor RNAs as indicated below. The binding mixtures were digested with RNase T_1 (0.05 U/10 μl) and analyzed by electrophoresis on a 6% nondenaturing polyacrylamide gel. Lane 1, free 3′ (+)487 RNA probe; lanes 2 and 9, 3′ (+)487 probes incubated in the absence of competitor RNA with mock- and MHV-infected lysates, respectively; lanes 3 and 10, in the presence of a 50-fold molar excess of unlabeled specific 3′ (+)487 RNA; lanes 4 and 11, in the presence of a 100-fold molar excess of unlabeled 3′ (+)487 RNA; lanes 5 and 12, in the presence of a 50-fold molar excess of nonspecific tRNA; lanes 6 and 13, in the presence of a 100-fold molar excess of tRNA; lanes 7 and 14, in the presence of a 50-fold molar excess of a 294-nt RNA from the 5′ end of the MHV-A59 genome; lanes 8 and 15, in the presence of a 100-fold molar excess of a 294-nt RNA from the 5′ end of the MHV-A59 genome. Arrowheads denote the positions of RNA-protein complexes. The material migrating at the bottom of the gel represents the digestion products from the nonprotected portions of the probe.

Localization of protein-binding sites at the 3′ end of JHM genomic RNA. From the results shown in Fig. 2, it appears that at least one protein-binding element is contained within the 3′ most 487 nt of the genome. Since two bands are visualized, it is possible that there are two different protein-binding elements, or alternatively a single protein-binding site could form different complexes with multiple proteins. To localize the

FIG. 3. Titration of RNase T_1 concentration for 3′ (+)84 RNA-protein binding. ^{32}P-labeled 3′ (+)84 RNA was incubated with uninfected-cell extracts at 22°C for 20 min. Binding mixtures were then digested at 22°C for 20 min in 10-μl reactions using decreasing amounts of RNase T_1. Lane 1, 0.05 U; lane 2, 0.025 U; lane 3, 0.0125 U; lane 4, 0.00625 U; lane 5, 0.003125 U. The arrowhead indicates the RNA-protein complex.

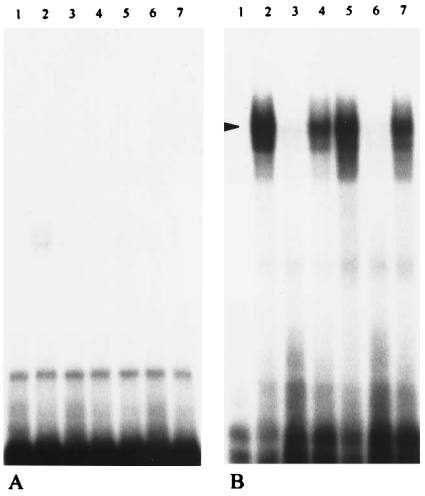

FIG. 4. Localization of the protein-binding site with 3′ (+)42 and 84-43 RNA probes. RNA-protein binding reactions were carried out as described in the legend to Fig. 2 except that RNase T_1 digestion was with 0.00625 U. (A) Lane 1, free 84-43 probe; lanes 2 and 5, 84-43 probes incubated in the absence of competitor RNA with mock- and MHV-infected lysates, respectively; lanes 3 and 6, 84-43 probes incubated in the presence of a 75-fold molar excess of unlabeled specific 3′ (+)84 RNA with mock- and MHV-infected lysates, respectively; lanes 4 and 7, 84-43 probes incubated in the presence of a 75-fold molar excess of nonspecific tRNA with mock- and MHV-infected lysates, respectively. (B) Lane 1, free 3′ (+)42 RNA probe; lanes 2 and 5, 3′ (+)42 probes incubated in the absence of competitor RNA with mock- and MHV-infected lysates, respectively; lanes 3 and 6, 3′ (+)42 probes incubated in the presence of a 75-fold molar excess of unlabeled specific 3′ (+)84 RNA with mock- and MHV-infected lysates, respectively; lanes 4 and 7, 3′ (+)42 probes incubated in the presence of a 75-fold molar excess of nonspecific tRNA with mock- and MHV-infected lysates, respectively.

region(s) on the 3′ (+)487 RNA probe with which the cellular protein(s) may associate, a set of deleted, ^{32}P-labeled RNA probes corresponding to various portions of the 3′ (+)487 RNA was synthesized in vitro (Fig. 1) and tested for the ability to form RNA-protein complexes. Using 0.05 U of RNase T_1 for limited digestion per 10-μl reaction, we demonstrated the specific formation of RNase T_1-resistant complexes with probes representing the 3′-most 333, 171, and 113 nt of the MHV genome (data not shown). These results are summarized in Fig. 1. These experiments mapped the binding site to within 113 nt from the 3′ end of the genomic RNA. However, variable results were observed when a shorter 3′ (+)84 probe was used; i.e., no complex formed in one experiment, and weak protein binding was observed in another (data not shown). To examine the possibility that shortening the probe to 84 nt lowered the binding affinity of proteins to the probe, either by altering the stability of the structure needed for protein binding or by deleting one of several elements involved in protein binding, we determined if digestion with lesser amounts of RNase T_1 would allow us to visualize formation of less stable RNA-protein complexes. As shown in Fig. 3, RNA-protein complexes could be visualized with the 3′ (+)84 probe when the concentration of T_1 was less than 0.0125 U/10-μl reaction. Here we especially emphasize that titration of the T_1 in these digestions is critical to detect weak binding activity. Therefore, we have titered the T_1 concentration for each deleted probe to select optimal concentrations for digestion. To further define the sequence responsible for protein binding, two probes, 84-43 and 3′ (+)42, representing each half of the 3′ (+)84 RNA, were synthesized and examined for the ability to form complexes with cytoplasmic extracts. A single complex was observed with the ^{32}P-labeled 3′ (+)42 probe (Fig. 4B), but no complex could be detected with the 84-43 probe (Fig. 4A). Consistent with this result is the finding that only the unlabeled 3′ (+)84 probe, not the nonspecific tRNA, can compete with ^{32}P-labeled 3′ (+)42 probe for protein binding (Fig. 4B). These results mapped a protein-binding element within the 42 nt at the 3′ end of JHM genomic RNA.

The fact that we observed two complexes in reactions containing the 3′ (+)487 RNA and host cell proteins, whereas a single complex formed with the 3′ (+)84 RNA, led us to search for the possible existence of other protein-binding elements at the 3′ end of JHM genomic RNA. For this purpose, cross-competition assays were first performed with ^{32}P-labeled 3′ (+)84 and 3′ (+)487 probes to assay their relative abilities to bind host cell proteins in the presence of both unlabeled 3′ (+)84 and 3′ (+)487 competitor RNAs (Fig. 5). No difference was observed when a 0.1- to 1-fold molar excess of either unlabeled 3′ (+)84 or 3′ (+)487 was used to compete with ^{32}P-labeled 3′ (+)84 (Fig. 5A) and ^{32}P-labeled 3′ (+)487 (Fig. 5B). With the ^{32}P-labeled 3′ (+)84 probe, the formation of RNase T_1-resistant complexes was completely blocked in the presence of a 100- to 200-fold molar excess of either unlabeled 3′ (+)84 or 3′ (+)487 RNA but not in the presence of nonspecific competitor tRNA (Fig. 5A). While the formation of complexes with ^{32}P-labeled 3′ (+)487 was completely blocked with unlabeled 100- to 400-fold-molar-excess 3′ (+)487 RNA, it was barely affected by adding the same molar excess of unlabeled 3′ (+)84 RNA and nonspecific tRNA (Fig. 5B). This result implied the possible presence of some other binding site(s) upstream of 84 nt from the 3′ end of the JHM genomic RNA. Protein-binding elements upstream of nt 84 were sought in an RNase protection/gel mobility shift assay using a probe spanning nt 487 to 85. Two complexes similar in pattern to those observed with 3′ (+)487 were formed. These complexes were demonstrated to represent specific protein binding to the

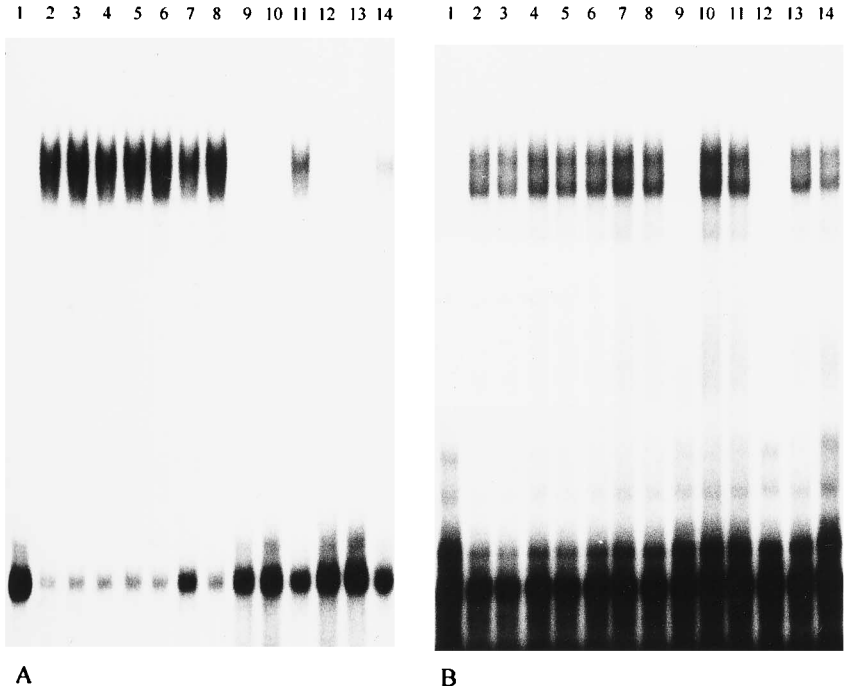

FIG. 5. Cross-competition assays of 3′ (+)84 RNA and 3′ (+)487 RNA. RNA-protein binding reactions were carried out as described in the legend to Fig. 2. (A) One nanogram of labeled 3′ (+)84 RNA was incubated with 7 μg of mock-infected cell lysate in the presence of competitor RNA and subsequently digested with 0.00625 U of RNase T_1. Lane 1, free probe; lane 2, probe with no competitor RNA; lanes 3 to 5, 0.1-fold molar excess of unlabeled 3′ (+)84, 3′ (+)487, and tRNAs, respectively; lanes 6 to 8, 1-fold molar excess of unlabeled 3′ (+)84, 3′ (+)487, and tRNAs, respectively; lanes 9 to 11, 100-fold molar excess of unlabeled 3′ (+)84, 3′ (+)487, and tRNAs, respectively; lanes 12 to 14, 200-fold molar excess of unlabeled 3′ (+)84, 3′ (+)487, and tRNAs, respectively. (B) One nanogram of labeled 3′ (+)487 RNA was incubated with 7 μg of mock-infected cell lysate in the presence of competitor RNA and subsequently digested with 0.05 U of RNase T_1. Lane 1, free probe; lane 2, probe with no competitor RNA; lanes 3 to 5, 0.1-fold molar excess of unlabeled 3′ (+)487, 3′ (+)84, and tRNAs, respectively; lanes 6 to 8, 1-fold molar excess of unlabeled 3′ (+)487, 3′ (+)84, and tRNAs, respectively; lanes 9 to 11, 100-fold molar excess of unlabeled 3′ (+)487, 3′ (+)84, and tRNAs, respectively; lanes 12 to 14, 400-fold molar excess of unlabeled 3′ (+)487, 3′ (+)84, and tRNAs, respectively.

RNA since a 150-fold molar excess of unlabeled tRNA did not block the binding, whereas the same molar excess of unlabeled specific competitor RNA (487-85) completely inhibited the formation of the RNase-resistant complexes (data not shown). Using a set of RNA probes containing deletions at the 5′ end (Fig. 1), we mapped the binding site to a sequence between nt 171 to 85 (data not shown). These experiments are summarized in Fig. 1. These results confirm that 487 bases within the 3′ end of JHM genomic RNA contain two protein-binding elements, which are localized separately between nt 42 and 1 and nt 171 and 85 (Fig. 1).

Characterization of binding proteins by UV-induced cross-linking. To characterize the protein(s) bound to the 3′ end of genomic RNA of MHV and determine their molecular weights, ^{32}P label was transferred from RNA probes to proteins bound directly to these RNAs by UV irradiation. After RNase T_1 limited digestion, RNA binding reaction mixtures were irradiated with UV light for 30 min and then completely digested with RNase A. Proteins to which ^{32}P label was transferred by cross-linking were analyzed by SDS-polyacrylamide gel electrophoresis (PAGE) through 12% polyacrylamide gels. No bands were observed after UV irradiation of RNA probes in the absence of cytoplasmic extracts (Fig. 6A, lanes 1 and 4; Fig. 6B, lane 1). As shown in Fig. 6A (lanes 2 and 3), the RNA-protein complex formed with 3′ (+)42 RNA contains approximately five host polypeptides, a highly labeled protein of 120 kDa and four minor species with sizes of 103, 81, 70, and 55 kDa. No protein bands were visualized when the same cytoplasmic extracts was incubated with the 84-43 probe (Fig. 6A, lanes 5 and 6). This result is consistent with the results of the gel mobility shift assay (Fig. 4). The second protein-binding element, contained within a probe representing nt 487 to 85 from the 3′ end of the genome, also labeled five host polypeptides of 142, 120, 100, 55, and 33 kDa in size, with the 120-kDa protein appearing to be the major protein component in the complex (Fig. 6B, lanes 2 and 3). However, some additional faint and indistinct bands were also sometimes observed. An example of such a band can be seen between the 50- and 35.1-kDa markers. We are unsure of the significance of these bands. When a 3′ (+)487 probe was used, the pattern with protein bands was similar to that obtained with the 487-85 RNA. As the signal that we obtained was very weak for the 3′ (+)487 RNA-protein complex after complete digestion of RNase A, we repeated this experiment using RNase T_1 for complete digestion after UV cross-linking. The same protein profiles were obtained (data not shown). Since the efficiency of UV cross-linking for different proteins to the RNA is highly variable (33), it is possible that the weak transfer of ^{32}P label to the minor bands is due to particularly low efficiency of cross-linking, or it could reflect a relatively low quantity of these proteins in the complexes. Although the complexes formed with the 3′ (+)42 RNA and the 487-85 RNA both contained 120- kDa and 55-kDa polypeptides, we are not sure whether these represent the same proteins contributing to complexes formed on separate sites. It is also possible that the 3′ (+)42 probe labeled a 142-kDa protein similar to that observed with the 487-85 RNA, but it was obscured by the heavy labeling and diffuseness of the 120-kDa protein in Fig. 6A. We have been unable to unequivocally resolve this question by repeated experiments and shorter exposures of the autoradiographs. In

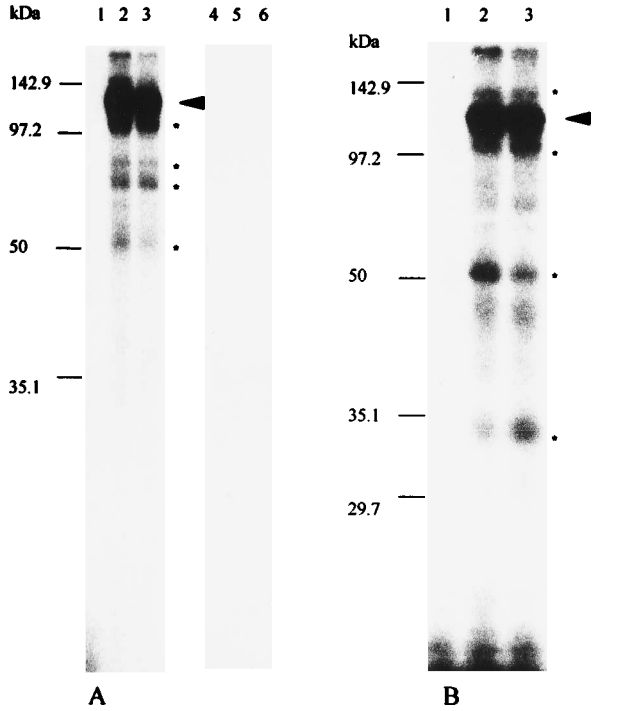

FIG. 6. Identification of host cell proteins binding to the 3′ end of MHV genomic RNA by UV cross-linking. RNA-protein binding reactions using labeled RNA were carried out as described in the legend to Fig. 2. Following incubation with RNase T_1 [0.00625 U for the 3′ (+)42 and 84-43 probes; 0.025 U for the 487-85 probe], ^{32}P-labeled RNA-protein complexes were UV cross-linked and digested with RNase A prior to SDS-PAGE (12% polyacrylamide gel). (A) Lane 1, free 3′ (+)42 probe; lane 2, 3′ (+)42 probe with mock-infected cell lysate; lane 3, 3′ (+)42 probe with MHV-infected cell lysate; lane 4, free 84-43 probe; lane 5, 84-43 probe with mock-infected lysate; lane 6, 84-43 probe with MHV-infected lysate. A highly labeled protein of 120 kDa is indicated by an arrowhead, and four minor proteins are indicated by asterisks. (B) Lane 1, free 487-85 probe; lane 2, 487-85 probe with mock-infected lysate; lane 3, 487-85 probe with MHV-infected lysate. A highly labeled protein of 120 kDa is indicated by an arrowhead; four minor proteins are indicated by asterisks. Prestained molecular weight standards (Bio-Rad) were used as markers.

addition, specific binding or complex formation was indeed mediated by protein in the cell lysates, since protein bands were no longer observed when the reaction mixture was incubated with proteinase K (1.5 mg/ml at 37°C for 1 h) after UV cross-linking and just prior to SDS-PAGE (data not shown). UV irradiation was necessary to transfer ^{32}P from RNA to protein; the identical procedure without UV irradiation did not result in any RNA-protein cross-linking (data not shown). The protein profiles obtained with JHM-infected cytoplasmic extracts were identical to those observed with uninfected cell extracts and the 3′ (+)42, 84-43, and 487-85 probes (Fig. 6).

DISCUSSION

Our approach to begin understanding the mechanism of MHV RNA replication is to precisely identify host and/or viral protein binding elements at the 3′ end of the genomic RNA, to characterize the RNA sequences and secondary structures responsible for the RNA-protein interactions, and to identify the proteins which bind to these elements. In this study, we report several findings that may give some insight into the requirements at the 3′ end of the genomic MHV RNA for replication. First, we have demonstrated that cytoplasmic proteins from host 17Cl-1 cells bind to the 3′ region of the positive-strand MHV RNA. The RNA-protein binding is specific, since a 50- to 100-fold molar excess of unlabeled probes blocked the formation of complexes, while nonspecific competitors did not. Lysates prepared from uninfected and MHV-infected cells gave identical patterns of RNase T_1-resistant complexes, and these complexes had identical protein profiles. Second, we mapped the RNA-binding elements to two regions of 42 and 86 nt within 3′-most 436 nt of genomic RNA, which is reported as the minimal length of sequence required for DI RNA replication (21). Finally, by using sequential and complete RNase digestion and UV cross-linking followed by SDS-PAGE, we were able to determine the apparent molecular masses of multiple proteins cross-linked to RNA.

During MHV replication in infected cells, the RNA polymerase complex starts from the positive-strand genomic 3′ end and transcribes a full-length copy of negative-strand RNA (1, 11, 36). It appears to transcribe subgenome-length negative-strand RNA as well (34). These negative-strand RNAs are the templates from which seven or eight species of positive-strand virus-specific RNAs with a 3′-coterminal nested-set structure are synthesized (9, 10, 17, 18, 35). Thus, synthesis of negative-strand RNA is a crucial early event in viral replication. If this event is blocked, virus replication will not proceed past the translation of input viral genomic RNA. Because of the large size of coronavirus genome RNA (about 31 kb) and unavailability of a full-length infectious cDNA clone, cDNA clones corresponding to replication-competent MHV DI RNAs have been created and extensively used to study the sequences required for MHV replication (6–8, 21, 22). Such a strategy has also been applied to identify the *cis*-acting replication signals in other positive-strand viruses such as Sindbis virus (20, 39) and brome mosaic virus (4). Deletions constructed in vitro have allowed the identification of the minimal sequences necessary for MHV DI RNA replication in the presence of helper virus. At least 436 bases derived from the 3′ end of the genome are required for replication (7, 21).

A recent study has further characterized the *cis*-acting elements required for MHV replication. In part on the basis of studies of other positive- and negative-strand viruses, protein-binding elements were sought within both the 5′ and 3′ termini of the MHV genome, and binding of a 55-kDa host cell protein to positive-strand RNA corresponding to nt 56 to 112 at the 5′ end of the genome was detected (5). The biological role of this 55-kDa protein in viral replication is unknown. Experiments using a 90-base probe spanning the 3′ terminus of the genomic RNA of positive sense failed to demonstrate any protein binding (5), which differs from our results reported here. This difference is probably due to the relatively low affinity binding of host proteins to the 3′ end of genomic RNA compared with the binding of host proteins to the 5′ end of the genome (41), combined with the different methodologies used by the two studies. The addition of an RNase T_1 digestion step increases the sensitivity and specificity of the assay that we used compared to simple mobility shift assays (14).

Host cell proteins binding to either the 3′ or the 5′ end of genome RNA have been reported in positive-strand rubella virus (26), poliovirus (24, 25), and hepatitis A virus (28) as well as in negative-strand measles virus (19). Host proteins were also found to bind to multiple sites at the 5′-end genome of positive-strand poliovirus (2) and at the 3′ end of the full-length negative-sense Sindbis virus-specific RNA (30, 31). Although the definite biological role of these proteins in RNA replication has not been clarified, the interaction of host proteins with viral genomes has been suggested to be an important step in viral RNA replication (5, 19, 25, 26, 30, 31). At present little is known regarding host and virus-specific factors in the RNA-dependent RNA polymerase complex necessary for ini-

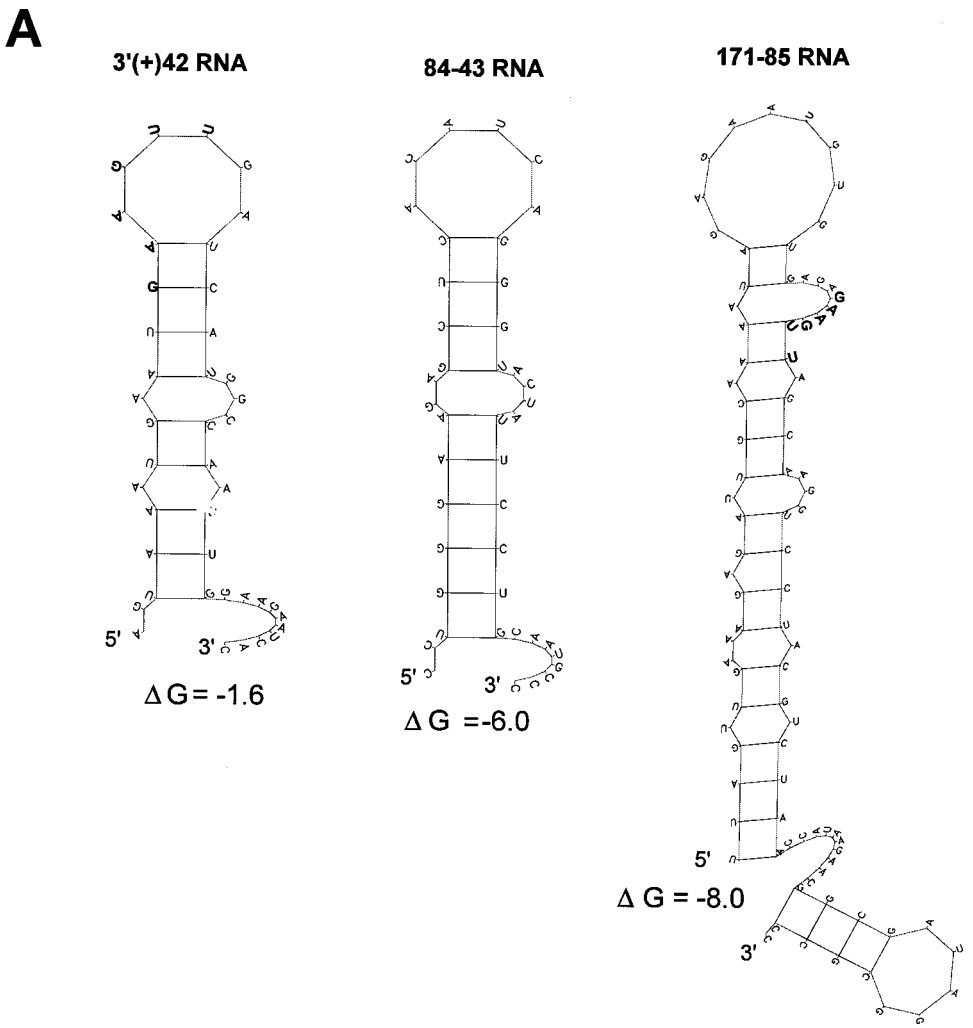

FIG. 7. Secondary structure prediction and sequence comparison of protein-binding segments. (A) Secondary structure predictions of 3′ (+)42, 84-43, and 171-85 RNAs were made by using the RNAFOLD program. The free energy of the stem-loop structure at each site is given in kilocalories per mole (1 kcal = 4.184 kJ). The position of the sequence GAAGUU, which is present in both 3′ (+)42 and 171-85 probes, is indicated with boldface letters. (B) The RNA sequences of nt 42 to 1 and nt 171 to 85 from the 3′ end of the JHM genome were aligned by using the GAP program. The sequence GAAGUU is present in both elements (marked with a box).

tiation of negative-strand RNA synthesis during MHV RNA replication.

The data reported here suggest that host cell proteins probably are involved in MHV RNA replication. Fine deletion analysis demonstrated that the replication of DI RNA could not occur if sequences from nt 107 to 16 or 267 to 90 from the 3′ end of the genome were deleted (7). Both sequences contain portions of protein-binding elements that we mapped, i.e., nt 42 to 1 and 171 to 85, and this finding further supports the possible role of binding of host cell proteins to the 3′ end of the genome in MHV RNA replication. All of our RNase protection/gel retardation and UV cross-linking experiments to date have failed to demonstrate binding of a virus-specific protein to the 3′ end of the MHV genome, yet the MHV RNA-dependent RNA polymerase must recognize this region of the genome to initiate negative-strand RNA synthesis. This may be an indication that viral proteins do not bind directly to the genomic RNA but associate with protein-binding elements within genomic RNA indirectly via protein-protein interactions and thus might not be detected by the UV cross-linking assay described here. Alternatively, it might be that the binding affinity of viral protein to RNA is so low that the RNA-protein complex formed with MHV polymerase proteins is not resistant to RNase T_1 digestion under any of the conditions that we used. The results of our UV cross-linking experiment indicate that the 42-1 and 487-85 protein-binding elements each bind proteins of 120 and 55 kDa. We have not yet determined if this represents binding of the same two proteins to both elements or if these proteins coincidently have similar electrophoretic mobilities.

RNA sequence elements with protein-binding activity often contain secondary structures (23, 27). Analysis of the 3′-most 487 nt of the MHV-JHM genome by using the Fold program in the University of Wisconsin Genetics Computer Group se-

quence analysis package indicates the potential formation of multiple stem-loop structures in this region. The sequence in this region is highly conserved among various strains of MHV (32). Predictions of secondary structure with RNA probes 3′ (+)42, 171-85, and 84-43, of which the former two are sites for host cell protein binding and the latter are not, revealed that each RNA is predicted to contain potential stem-loop structures, although these structures are not predicted to be particularly stable (Fig. 7A). We compared the sequences of two protein-binding elements, 171-85 and 3′ (+)42, and about 42% sequence identity was found, with the sequence GAAGUU being present in both elements (Fig. 7B). This sequence is fully conserved among MHV strains. For both the 3′ (+)42 and the 171-85 elements, this sequence is predicted to be largely nonbase paired, either as a bulge in a stem or a bulge in a loop (Fig. 7A). Future studies will be directed to determine the precise sequence and secondary structure required for host protein binding.

ACKNOWLEDGMENTS

We especially thank Ann-Bin Shyu of the Department of Biochemistry for valuable advice and instruction on gel mobility shift and UV cross-linking techniques. We thank Brenda Hogue of Baylor College of Medicine for critical reading and helpful comments on the manuscript. We thank Robin Stalcup for preparing MHV-JHM virus stocks and all members of the Leibowitz laboratory for helpful discussion.

This work was supported by National Multiple Sclerosis Society research grant RG 2203-A-5 and by a grant from the Texas Advanced Research Program.

REFERENCES

1. **Baric, R. S., S. A. Stohlman, and M. M. C. Lai.** 1983. Characterization of replicative intermediate RNA of mouse hepatitis virus: presence of leader RNA sequences on nascent chains. J. Virol. **48:**630–663.
2. **Del Angel, R. M., A. G. Papavassiliou, C. Fernandez-Tomas, S. J. Silverstein, and V. R. Racaniello.** 1989. Cell proteins bind to multiple sites within the 5′ untranslated region of poliovirus RNA. Proc. Natl. Acad. Sci. USA **86:**8299–8303.
3. **Dignam, J. D., R. M. Lebovitz, and R. G. Roeder.** 1983. Accurate transcription initiation by RNA polymerase II in a soluble extract from isolated mammalian nuclei. Nucleic Acids Res. **11:**1475–1489.
4. **French, R., and P. Ahlquist.** 1987. Intercistronic as well as terminal sequences are required for efficient amplification of brome mosaic virus. J. Virol. **61:**1457–1465.
5. **Furuya, T., and M. M. C. Lai.** 1993. Three different cellular proteins bind to complementary sites on the 5′-end-positive and 3′-end-negative strands of mouse hepatitis virus RNA. J. Virol. **67:**7215–7222.
6. **Furuya, T., T. B. Macnaughton, N. La Monica, and M. M. C. Lai.** 1993. Natural evolution of coronavirus defective-interfering RNA involves RNA recombination. Virology **194:**408–413.
7. **Kim, Y. N., Y. S. Jeong, and S. Makino.** 1993. Analysis of *cis*-acting sequences essential for coronavirus defective interfering RNA replication. Virology **197:**53–63.
8. **Kim, Y. N., M. M. C. Lai, and S. Makino.** 1993. Generation and selection of coronavirus defective interfering RNA with large open reading frame by RNA recombination and possible editing. Virology **194:**244–253.
9. **Lai, M. M. C.** 1990. Coronavirus: organization, replication and expression of genome. Annu. Rev. Microbiol. **44:**303–333.
10. **Lai, M. M. C., P. R. Brayton, R. C. Armen, C. D. Patton, C. Pugh, and S. A. Stohlman.** 1981. Mouse hepatitis virus A59: mRNA structure and genetic localization of the sequence divergence from hepatotropic strain MHV-3. J. Virol. **39:**823–834.
11. **Lai, M. M. C., C. D. Patton, and S. A. Stohlman.** 1982. Replication of mouse hepatitis virus: negative-stranded RNA and replicative-form RNA are of genome length. J. Virol. **44:**487–492.
12. **Lai, M. M. C., and S. A. Stohlman.** 1978. RNA of mouse hepatitis virus. J. Virol. **26:**236–242.
13. **Lee, H.-J., C.-K. Shieh, A. E. Gorbalenya, E. V. Koonin, N. LaMonica, J. Tuler, A. Bagdzhadzhyan, and M. M. C. Lai.** 1989. The complete sequence (22 kilobases) of murine coronavirus gene-1 encoding the putative proteases and RNA polymerase. Virology **180:**567–582.
14. **Leibold, E. A., and H. N. Munro.** 1988. Cytoplasmic protein binds in vitro to a highly conserved sequence in the 5′ untranslated region of ferritin heavy- and light-subunit mRNAs. Proc. Natl. Acad. Sci. USA **85:**2171–2175.
15. **Leibowitz, J. L., and J. R. DeVries.** 1988. Synthesis of virus-specific RNA in permeabilized murine coronavirus-infected cells. Virology **166:**66–75.
16. **Leibowitz, J. L., S. R. Weiss, E. Paavola, and C. W. Bond.** 1982. Cell-free translation of murine coronavirus RNA. J. Virol. **43:**905–913.
17. **Leibowitz, J. L., K. C. Wilhelmsen, and C. W. Bond.** 1981. The virus-specific intracellular RNA species of two murine coronaviruses: MHV-A59 and MHV-JHM. Virology **114:**39–51.
18. **Leibowitz, J. L., P. W. Zoltick, K. V. Holmes, E. L. Oleszak, and S. R. Weiss.** 1990. Murine coronavirus RNA synthesis, p. 67–74. *In* M. A. Brinton and F. X. Heinz (ed.), New aspects of positive-strand RNA viruses. American Society for Microbiology, Washington, D.C.
19. **Leopardi, R., V. Hukkanen, R. Vainionpaa, and A. A. Salmi.** 1993. Cell proteins bind to sites within the 3′ noncoding region and the positive-strand leader sequence of measles virus RNA. J. Virol. **67:**785–790.
20. **Levis, R., B. W. Weiss, M. Tsiang, H. Huang, and S. Schlesinger.** 1986. Deletion mapping of Sindbis virus DI RNAs derived from cDNAs defines the sequences essential for replication and packaging. Cell **44:**137–145.
21. **Lin, Y. J., and M. M. C. Lai.** 1993. Deletion mapping of a mouse hepatitis virus defective interfering RNA reveals the requirement for an internal and discontiguous sequence for replication. J. Virol. **67:**6110–6118.
22. **Makino, S., C. K. Shieh, L. H. Soe, S. C. Baker, and M. M. C. Lai.** 1988. Primary structure and translation of a defective interfering RNA of murine coronavirus. Virology **166:**550–560.
23. **Mattaj, I. W.** 1993. RNA recognition: a family matter? Cell **73:**837–840.
24. **Meerovitch, K., J. Pelletier, and N. Sonenberg.** 1989. A cellular protein that binds to the 5′-noncoding region of poliovirus RNA: implications for internal translation initiation. Genes Dev. **3:**1026–1034.
25. **Najita, L., and P. Sarnow.** 1990. Oxidation-reduction sensitive interaction of a cellular 50-KDa protein with an RNA hairpin in the 5′ noncoding region of the poliovirus genome. Proc. Natl. Acad. Sci. USA **87:**5846–5850.
26. **Nakhasi, H., X. Q. Cao, T. A. Rouault, and T. Y. Liu.** 1991. Specific binding of host cell proteins to the 3′-terminal stem-loop structure of rubella virus negative-strand RNA. J. Virol. **65:**5961–5967.
27. **Nakhasi, H. L., T. A. Rouault, D. J. Haile, T. Y. Liu, and R. D. Klausner.** 1990. Specific high-affinity binding of host cell proteins to the 3′ region of rubella virus RNA. New Biol. **2:**255–264.
28. **Nuesch, J. P. F., M. Weitz, and G. Siegl.** 1993. Proteins specifically binding to the 3′ untranslated region of hepatitis A virus RNA in persistently infected cells. Arch. Virol. **128:**65–79.
29. **Pachuk, C. J., P. J. Breedenbeek, P. W. Zoltick, W. J. M. Spaan, and S. R. Weiss.** 1989. Molecular cloning of the gene encoding the putative polymerase of mouse hepatitis coronavirus strain A59. Virology **171:**141–148.
30. **Pardigon, N., E. Lenches, and J. H. Strauss.** 1993. Multiple binding sites for cellular proteins in the 3′ end of Sindbis alphavirus minus-sense RNA. J. Virol. **67:**5003–5011.
31. **Pardigon, N., and J. H. Strauss.** 1992. Cellular proteins bind to the 3′ end of Sindbis virus minus-strand RNA. J. Virol. **66:**1007–1015.
32. **Parker, M. M., and P. S. Masters.** 1990. Sequence comparison of the N genes of five strains of the coronavirus mouse hepatitis virus suggests a three domain structure for the nucleocapsid protein. Virology **179:**463–468.
33. **Pino-Roma, S., S. A. Adam, Y. D. Choi, and G. Dreyfuss.** 1989. Ultraviolet-induced cross-linking of RNA to proteins in vivo. Methods Enzymol. **180:**410–418.
34. **Sawicki, S. G., and D. L. Sawicki.** 1990. Coronavirus transcription: subgenomic mouse hepatitis virus replicative intermediates function in RNA synthesis. J. Virol. **64:**1050–1056.
35. **Spaan, W. J., D. Cavanagh, and M. C. Horzinek.** 1988. Coronaviruses: structure and genome expression. J. Gen. Virol. **69:**2939–2952.
36. **Spaan, W. J., P. J. Rottier, M. C. Horzinek, and B. A. Vander Zeust.** 1982. Sequence relationships between the genome and the intracellular RNA species 1, 3, 6, and 7 of mouse hepatitis virus strain A59. J. Virol. **42:**432–439.
37. **Sturman, L. S., and K. K. Takemoto.** 1972. Enhanced growth of a murine coronavirus in transformed mouse cells. Infect. Immun. **6:**501–507.
38. **Wege, H., A. Muller, and V. ter Meulen.** 1978. Genomic RNA of the murine coronavirus JHM. J. Gen. Virol. **41:**217–227.
39. **Weiss, B., H. Nitschko, I. Ghattas, R. Wright, and S. Schlesinger.** 1989. Evidence for specificity in the encapsidation of Sindbis virus RNAs. J. Virol. **63:**5310–5318.
40. **You, Y., C. Y. A. Chen, and A. B. Shyu.** 1992. U-rich sequence-binding proteins interacting with a 20-nucleotide U-rich sequence in the 3′ untranslated region of c-*fos* mRNA may be involved in the first step of c-*fos* mRNA degradation. Mol. Cell. Biol. **12:**2931–2940.
41. **Yu, W., and J. L. Leibowitz.** Unpublished data.